

Available online at [www.sciencedirect.com](http://www.sciencedirect.com)

ScienceDirect

journal homepage: [www.jfda-online.com](http://www.jfda-online.com)

## Original Article

# HPTLC-FLD-SERS as a facile and reliable screening tool: Exemplarily shown with tyramine in cheese



Liao Wang <sup>a,b,c</sup>, Xue-Ming Xu <sup>a,b,c</sup>, Yi-Sheng Chen <sup>a,b,c,\*</sup>, Jie Ren <sup>d</sup>,  
Yun-Tao Liu <sup>e</sup>

<sup>a</sup> State Key Laboratory of Food Science and Technology, Jiangnan University, Wuxi 214122, China

<sup>b</sup> School of Food Science and Technology, Jiangnan University, Wuxi 214122, China

<sup>c</sup> Collaborative Innovation Center of Food Safety and Quality Control in Jiangsu Province, Jiangnan University, Wuxi 214122, China

<sup>d</sup> Nanchong Food and Drug Administration, Nanchong 637100, China

<sup>e</sup> College of Food Science, Sichuan Agricultural University, Yaan 625014, China

## ARTICLE INFO

## Article history:

Received 26 June 2017

Received in revised form

26 July 2017

Accepted 30 July 2017

Available online 18 August 2017

## Keywords:

FLD

HPTLC

SERS

Screening

Tyramine

## ABSTRACT

The serious cytotoxicity of tyramine attracted marked attention as it induced necrosis of human intestinal cells. This paper presented a novel and facile high performance thin-layer chromatography (HPTLC) method tailored for screening tyramine in cheese. Separation was performed on glass backed silica gel plates, using methanol/ethyl acetate/ammonia (6/4/1 v/v/v) as the mobile phase. Special efforts were focused on optimizing conditions (substrate preparation, laser wavelength, salt types and concentrations) of surface enhanced Raman spectroscopy (SERS) measurements directly on plates after derivatization, which enabled molecule-specific identification of targeted bands. In parallel, fluorescent densitometry (FLD) scanning at 380–400 nm offered satisfactory quantitative performances (LOD 9 ng/zone, LOQ 17 ng/zone, linearity 0.9996 and %RSD 6.7). Including a quick extraction/cleanup step, the established method was successfully validated with different cheese samples, both qualitatively (straightforward confirmation) and quantitatively (recovery rates from 83.7 to 108.5%). Beyond this application, HPTLC-FLD-SERS provided a new horizon in fast and reliable screening of sophisticated samples like food and herb drugs, striking an excellent balance between specificity, sensitivity and simplicity.

Copyright © 2017, Food and Drug Administration, Taiwan. Published by Elsevier Taiwan LLC. This is an open access article under the CC BY-NC-ND license (<http://creativecommons.org/licenses/by-nc-nd/4.0/>).

\* Corresponding author. State Key Laboratory of Food Science and Technology, Jiangnan University, Wuxi 214122, China. Fax: +86 0510 85917100.

E-mail address: [chen.yisheng@jiangnan.edu.cn](mailto:chen.yisheng@jiangnan.edu.cn) (Y.-S. Chen).

<http://dx.doi.org/10.1016/j.jfda.2017.07.007>

1021-9498/Copyright © 2017, Food and Drug Administration, Taiwan. Published by Elsevier Taiwan LLC. This is an open access article under the CC BY-NC-ND license (<http://creativecommons.org/licenses/by-nc-nd/4.0/>).

## 1. Introduction

Nowadays, instrumentalized HPTLC was taking an increasingly elevating position over conventional HPLC/GC in food and drug screening [1–6]. In addition to its intrinsic merits like high throughput and user-friendliness purely as a separation tool, there was a trend to employ HPTLC as a flexible and matrix-robust platform simultaneously bridging a large array of advanced detectors like biosensors [7–9], MS [10,11] and NMR [12] at ease. This was shaping the future development of HPTLC, which would substantially strengthen and expanded its applicability.

Coupling surface enhanced Raman spectroscopy (SERS) with HPTLC was proposed shortly after the discovery of this abnormal optical phenomenon by Fleischmann in 1974, but initially not that successful due to hardware limitations. With the popularizing of portable Raman spectrometry, this analytical strategy became increasingly attractive, especially to controlling laboratories with limited resources. The featuring advantage of SERS was the sharp, fingerprint like spectra pattern specific to analyte at extremely low concentrations (even to a single molecule), making it one of the most dynamically developing frontier in analytical chemistry [13–17]. Nevertheless, SERS detection also faced difficulties with sophisticated samples like food. As it was known that the enhancement factors of SERS were critically dependent on the absorption of molecules to substrate surface. Therefore, food matrices with a stronger affinity towards substrate would subject to higher enhancement, flooding the weak signals by targeted compounds. When linked to HPTLC, this inefficiency of SERS would be substantially improved, since the analyte and matrices was physically isolated from each other after separation [17,18]. Obviously, HPTLC-SERS was a much more cost-effective alternative to HPTLC-MS/NMR in identifying chromatographic fingerprints.

Cheese, rich in protein, vitamins and many other health-beneficial nutrition, was becoming increasingly popular in many Asian countries. But growing attention had been paid to the toxicity risk posed by biogenic amines accumulated in the manufacturing process. Tyramine (Tyr) was the most abundant biogenic amine in cheese, which was mainly responsible for the “cheese effects” characterized with hypertension, headache or even migraine. Moreover, using real-time cell analysis it was recently revealed that Tyr can induce necrosis of human intestinal cells and this cytotoxicity was even stronger than that of histamine [19]. In order to ensure food safety, facile and reliable method for screening Tyr in cheese was urgently needed.

The specific objective of this work was to establish a real screening-tailored method for the reliable confirmation and quantitation of Tyr in cheese products, against the strictest maximum residue limit (MRL) established by EU [20]. To achieve this goal, bands visualized by fluorescamine was directly assayed by SERS and fluorescent densitometry (FLD). Meanwhile, special attention was focused on the key parameters (substrate preparation, laser wavelength, salt types and concentrations selection) tightly related to the detectability of SERS.

## 2. Methods

### 2.1. Chemicals

Tyramine hydrochloride (>98% purity) and fluorescamine (>99% purity) as well as methanol, ethyl acetate were purchased from Aladdin (Shanghai, China). Ultra-pure water was prepared by a Synergy system (Millipore, Schwalbach, Deutschland). Other chemicals and solvents of analytical grade were from Sigma Aldrich (Shanghai, China). Class backed silica gel F<sub>254</sub> plates (20 × 10 cm, analytical grade, serial No. 4022536067940) was supplied by Merck (Darmstadt, Deutschland). Prior using, each plate was pre-washed with methanol. All cheese samples were purchased at local supermarkets.

### 2.2. Standard solutions and samples preparation

The stock solution of Tyr was prepared by dissolving 10.0 mg reference standard with 10 mL methanol. Working solutions were 1:50 (for establishing the calibration curve) and 1:1000 (for determining method sensitivity) folds diluted with methanol.

Extraction and cleanup of Tyr from cheese matrix was principally based on the method described by Restuccia [21]. Briefly, 5.0 g chopped cheese was weighted in a 50.0 mL test tube filled with 20 mL of 0.1 mol/L hydrochloric acid. If necessary, the mixtures were spiked with 150 or 100 µL Tyr stock solution, resulting in 30 or 20 mg/kg artificially contamination. The suspension was mixed in ultrasonic bath (40 °C) for 5 min, homogenized by vortex for 3 min and then centrifuged at 10,000 g for 10 min at 4 °C. The obtained supernatant was used for analysis after filtering through a 0.45 µm membrane in a 5 mL syringe.

### 2.3. Microwave assisted AgNPs fabrication

Colloid of AgNPs was prepared via chemical reduction methods proposed by Lee and Meisel [22], but accelerated by using microwave irradiation as the heating method. Briefly, 45 mg AgNO<sub>3</sub> and 50 mg trisodium citrate was dissolved in 250 mL water. This mixture was heated at high power and monitored every 2 min. The morphology and surface charge of obtained AgNPs was characterized by a JEM-2100 transmission electronic microscopy (JEOL, Tokyo, Japan) and a Zetasizer (Malvern Instruments Ltd, Malvern, UK), respectively. Further, the crude colloid was 10 folds condensed by centrifuging.

### 2.4. Chromatography and derivatization

A TLC sampler Linomat 5 (CAMAG, Muttenz, Switzerland) was used to apply the sample liquid as 6 mm bands carried by a nitrogen gas stream, with position settings: 8 mm from the lower edge, 15 mm initially from the left side and track gap automatically calculated.

The chromatography was performed with an ADC-2 (CAMAG, Muttenz, Switzerland). In order to guarantee

straight and reproducible chromatographic results, following settings were used: 30 s pre-drying, 5 min humidity control (33%), 5 min tank saturation, 15 min plate pre-conditioning, 60 mm migration distance. Following a short heating at 100 °C to eliminate ammonia residue, analyte was fluorescently labeled by dipping the plate into 0.1 mg/mL fluorescamine in acetone with a TLC Immersion Device III (CAMAG, Muttenz, Switzerland) at a vertical speed of 2 cm/s and 2 s stay. After that, the plate was heated at 100 °C on a plate heater to visualize the analyte.

### 2.5. Plate documentation and densitometry

Digital images of the developed plates were captured by a DD70 imaging system (Biostep, Burkhardtendorf, Deutschland) under 366 nm light. Then, the plates were densitometrically scanned with a TLC Scanner 3 (CAMAG, Muttenz, Switzerland) in fluorescence mode with following settings: slit dimension 3.00 × 0.30 mm (Micro), optical system for maximum resolution, scanning speed 20 mm/s, data resolution 50 μm/step, mercury lamp 380<400 nm (K400 optical filter). Data acquisition and processing was done by CAMAG winCATS software in quantitative mode version 1.4.6.

### 2.6. HPTLC-SERS

Bands visible to naked eyes under 366 nm light was marked with a soft-pencil. To the center of these bands, AgNPs colloid (1 μL) and salt solutions (1 μL) at different concentrations were successively spotted. After that, the SERS spectra were immediately recorded with a Raman spectrometer (Horiba Jobin Yvon S.A.S, France) in reflection mode. To do so, bands of interest were manually adjusted on the sample stage guided by a red beam. Three laser sources including Nd:YAG 532 nm, He:Ne 633 nm and diode 785 nm was used for excitation and the laser beam was focused with a 100× objective in 90° geometry. For each SERS measurement, signal acquisition was averaged from three times accumulations of 10 s. The obtained data was process and quantified with LabSpec 5 software, 9.10.27 version.

## 3. Results and discussion

### 3.1. HPTLC-FLD optimization

To achieve acceptable separation of the analyte from other matrices which can also be visualized by derivatization, initially a large array of solvent systems was tested as mobile phase. After comparison, methanol/ethyl acetate/ammonia 6/4/1 (v/v/v) that delivered the best resolution was selected for following separations. As shown in Fig. 1A, a sharp window space (at  $R_f$  of 0.38) comparable for both the standard and positive finds in cheese samples was achieved after separation. The strictest MRL of Tyr for consumer taking classical MOID was established at 6 mg/kg [20], or 22.5 ng/band expressed as absolute quantity on TLC plates assuming 15 μL extract was applied. Here, the sensitivity of eye inspection was down to 20 ng/band. In another word, preliminary judgments on the non-compliance profile of samples can be easily

reached from visual impression, thus extremely valuable for screening work.

More accurate assessment was performed by densitometry in fluorescence mode. With the intension to fix the optimal excitation wavelength, the fluorescence spectrum (320–400 nm) of targeted bands was probed first. As depicted in Fig. 1S, it was clear that the profiles of obtained spectra displayed high similarity, reaching maxima at 380 nm. Combined with a K400 optical filter, this wavelength was found also suitable for matrix-matched runs, as shown in Fig. 1B.

### 3.2. HPTLC-SRES optimization

It was well accepted that metallic nanostructures as active substrates played a key role in SERS observation and a broad diversity of strategies had been proposed for their preparation. Nevertheless, a synthesis protocol that was simple, toxic-reagent-free and time-saving was highly favored from a practical perspective. Taking these factors into consideration, microwave irradiation was employed in this study to accelerate the preparation of Ag nanoparticles (AgNPs) via the classic reaction of citrate and AgNO<sub>3</sub>. It was clear from Fig. 2S-A that considerable AgNPs had been fabricated only after 6 min irradiation, reflected by the appearance of dark gray color of the solution. Zeta potential results and microscopic images confirmed the AgNPs obtained at this moment were negatively charged ( $-32.4 \pm 0.2$  mV) and of spherical shape as shown in Fig. 2S-B. But, it did not make sense to extend the reaction longer than 6 min, because flocculation occurred after that. Therefore, AgNPs after 6 min reaction was used for SERS detection.

In addition to the enhancement induced by active substrates, excitation wavelength was another crucial factor affecting the strength of SERS signals. Accumulated evidences indicated that resonant SERS phenomenon may occur on condition that the frequency of the laser matched the electronic transition resonance of the targeted compounds, resulting in substantial elevation of SERS signals [23]. Consequently, the usability of three different incident laser at 532, 633 and 785 nm, respectively, was assessed for SERS detection. Nevertheless, preliminary tests disclosed that the molecules of Tyr deposited on silica gel layer was “blind” to any incident laser, as shown in Fig. 3S. This implied that AgNPs alone was not able to trigger detectable SERS signals of analyte. Apart from that, another major obstacle of detection was the excessive fluorescamine resulted from dipping. Similar to our previous experiences, its presence led to strong background noises.

As highlighted in many reports associated with SERS, either with solutions or HPTLC plates, the adding of salts as activator was often of crucial importance for generating detectable signals [24–26]. Particularly, our previous study demonstrated that the presence of NaCl effectively suppressed noises due to excessive fluorescamine [27]. Inspired by these reports, a wide range of salts was investigated here, with regard to their efficacy to enhance the detectability of SERS and to remove the masking effects caused by excessive derivative reagent. Fig. 2 and Fig. 4S comparatively presented the SERS results of Tyr bands and the background, resulted from different combinations of aforementioned parameters. To our surprise, the effects of the 6 investigated salts on SERS

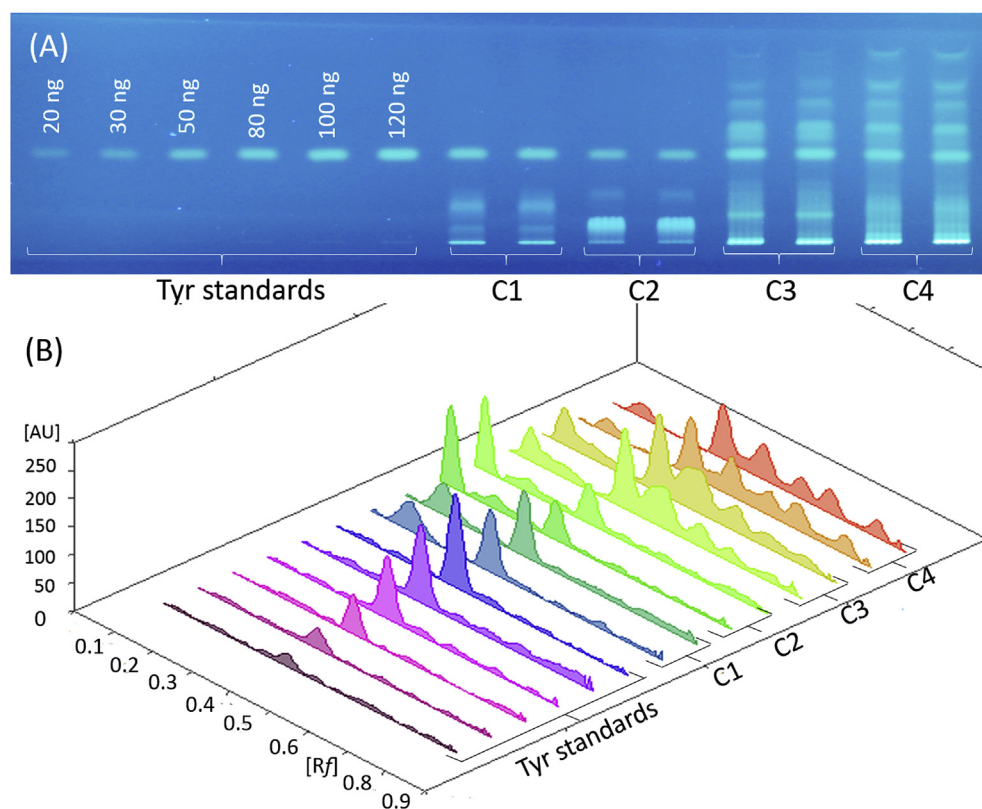


**Fig. 1 – Separation results of Tyr standard and cheese samples (A) and corresponding densitogram by FLD at 380–400 nm.**

differed dramatically, though they all showed excellent ability to wipe out background noises. More specifically, the addition of NaBr exclusively resulted in intensive and pattern-rich SERS fingerprints, regardless the variation of incident laser wavelengths; whereas insignificant enhancement was recorded at the presence of other 5 salts. This observation was contrary to previous reports in which NaCl unanimously offered the remarkable enhancement of SERS results [25,28], suggesting that the choosing of salts as SERS activator on HPTLC was not immutable but should be customized according to the molecular structures.

Conventional explanation of such salt-induced enhancement more emphasized the contribution by “hot spots” which are highly localized regions of intense local field enhancement. The chemical essence of “hot spots” is interstitial crevices between aggregated nano particles [29]. However, this theory was not able to convincingly explain why exclusively NaBr induced detectable SERS signals while the opposite was true for the other 5 salts that also can trigger aggregation of dispersed AgNPs. “Anion activation effect” offered an alternative explanation. It was assumed that anion (mainly  $\text{Cl}^-$ ) can mediate the formation of Ag-analyte complexes [24]. But our findings raised questions to this hypothesis. For instance, NaBr and KBr shared the same anion moiety, but their effects on SERS exhibited striking differences. This interesting discrepancy implied that the overall enhancement capacity of a salt should be attributed to the synergistic effects of both the anion and cation moieties, though the mechanism behind the difference was still not clear.

Furthermore, it was obvious that the use of different incident lasers led to remarkable variations of intensities and fingerprint patterns of the obtained SERS spectra. In comparison, the use of 633 nm laser offered superiorly more intensive and informative SERS results, which was characterized by a prominent peak at  $834\text{ cm}^{-1}$  and a peak cluster at  $1187$ ,  $1214$  and  $1243\text{ cm}^{-1}$ . With 532 nm excitation, the strongest peak shifted to  $815\text{ cm}^{-1}$  while the peak cluster at  $1215\text{ cm}^{-1}$  drastically attenuated. The SERS spectra obtained under 785 nm excitation exhibited a similar profile to that by 633 nm, however with the lowest overall intensity.

On this basis, the dose-effect of NaBr on SERS results was further quantitatively evaluated, with the intention to gain the highest signal enhancement. Here, different NaBr levels within the range of 0.1–4 mol/L was investigated. As shown in Fig. 3, the variation tendency of signal intensities obtained by 532 and 633 nm lasers displayed high similarity. More specifically, increasing amounts of NaBr from 0.1 to 3 mol/L benefited the intensification of SERS fingerprints, whereas a sharp decrease was observed at 4 mol/L. However, the performance of 633 nm laser was indeed better than that of 532 nm, evidenced by a superiorly stronger overall intensities of SERS spectra. Hence, 633 nm laser and 3 mol/L NaBr was selected for following experiments.

### 3.3. Method validation

Based on the aforementioned optimization, the potential of SERS as a quantitative tool was assessed, using FLD as the benchmark. As summarized in Table 1, it can be concluded

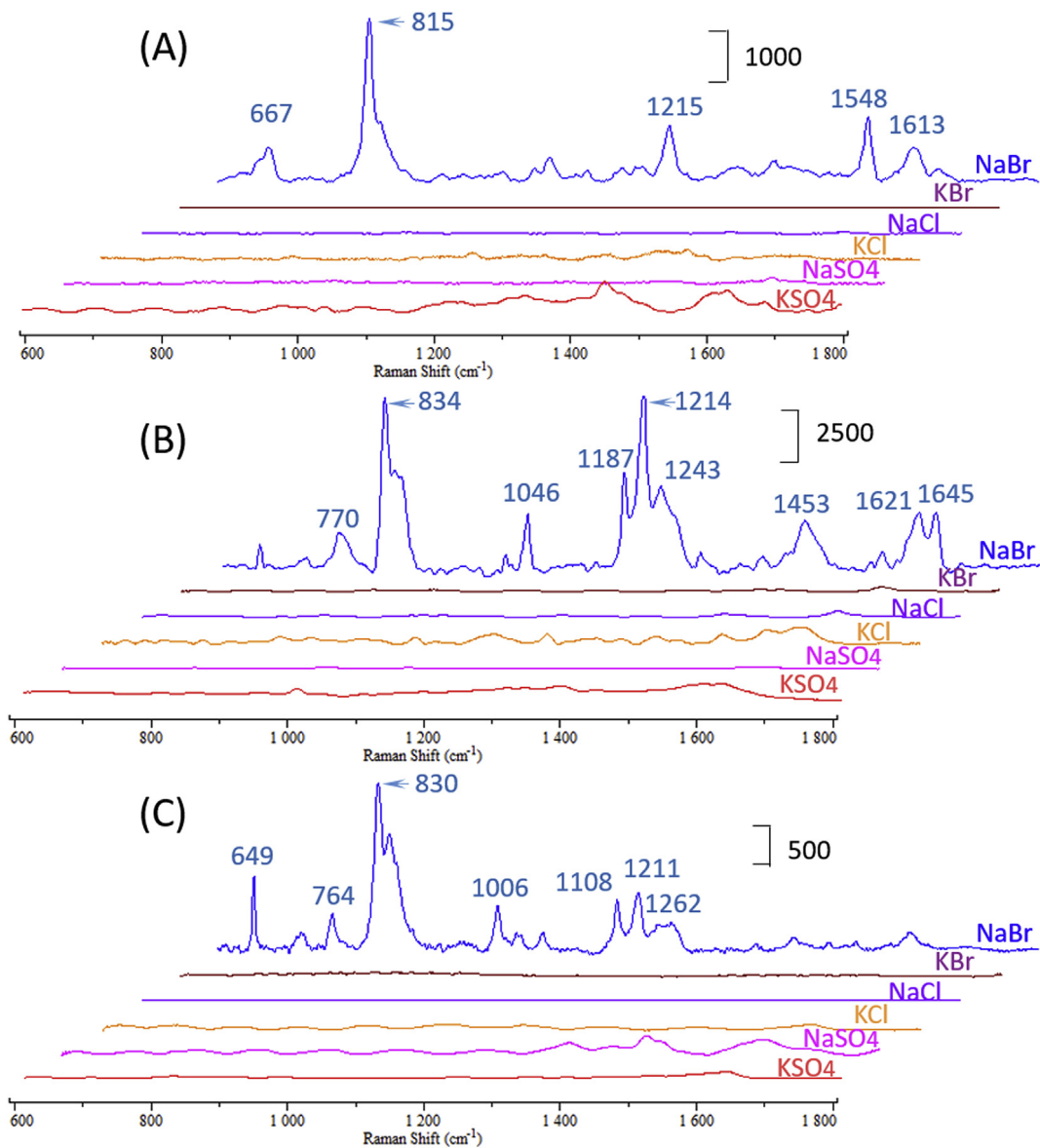


**Fig. 2** – AgNPs mediated SERS responses of Tyr bands after derivatization at the presence of different salts, excited by 532 (A), 633 (B) and 785 (C) nm lasers, respectively.

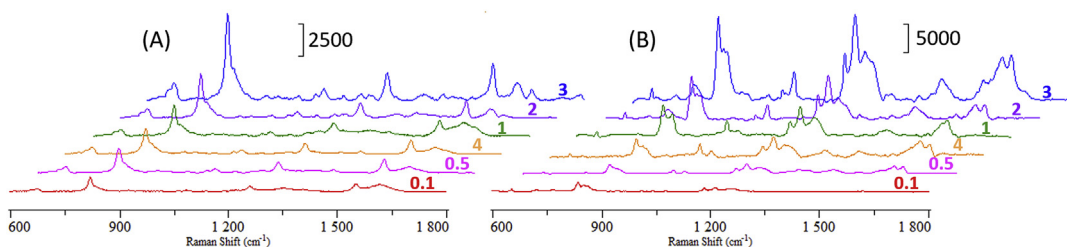


**Fig. 3** – Intensity variation profile of SERS fingerprints activated at different NaBr levels (mol/L), excited by 532 (A) and 633 (B) nm lasers, respectively.

that these two detections each showed superiorities in different aspects. Comparatively, SERS obviously offered better sensitivity than that of FLD, but not competitively quantifiable. However, such high sensitivity was not practically

attractive, since Tyr bands became invisible below 10 ng/band. On the other hand, FLD gave satisfactory linearity (0.9996) within the critical concentration range (20–120 ng/zone), while the precision was less than 7%. This implied that

**Table 1 – Comparison of the quantitative performances by different detection methods.**

Analytical parameters	FLD		SERS	
	380</400 nm	834 cm <sup>-1</sup>	1214 cm <sup>-1</sup>	
LOD (S/N 3, ng/band)	9	1	1	
LOQ (S/N 10, ng/band)	17	4	3	
Linearity (R <sup>2</sup> ) <sup>a</sup>	0.9996	0.9636	0.9452	
Precision (%RSD) <sup>b</sup>	6.7	11.6	13.9	

<sup>a</sup> Dynamic linearity was monitored within the range 20–120 ng/zone.  
<sup>b</sup> The precision was determined with zones of Tyr at 20 ng/band, n = 5.

the joint use of SERS as confirmative and FLD as qualitative tool, respectively, would facilitate the generation of more concrete results of screening.

To get matrix-tolerance proof of the established method, analysis was further carried out with cheese samples. Though the targeted bands were separated in a straight line, band assignment just according the R<sub>f</sub> was however not reliable. First, sample matrices of similar structures may overlap within targeted bands. Besides, the migration of analyte may shift at the presence of matrices, from our previous experiences. Keeping these concerns in mind, the SERS measurements were comparatively taken toward bands at

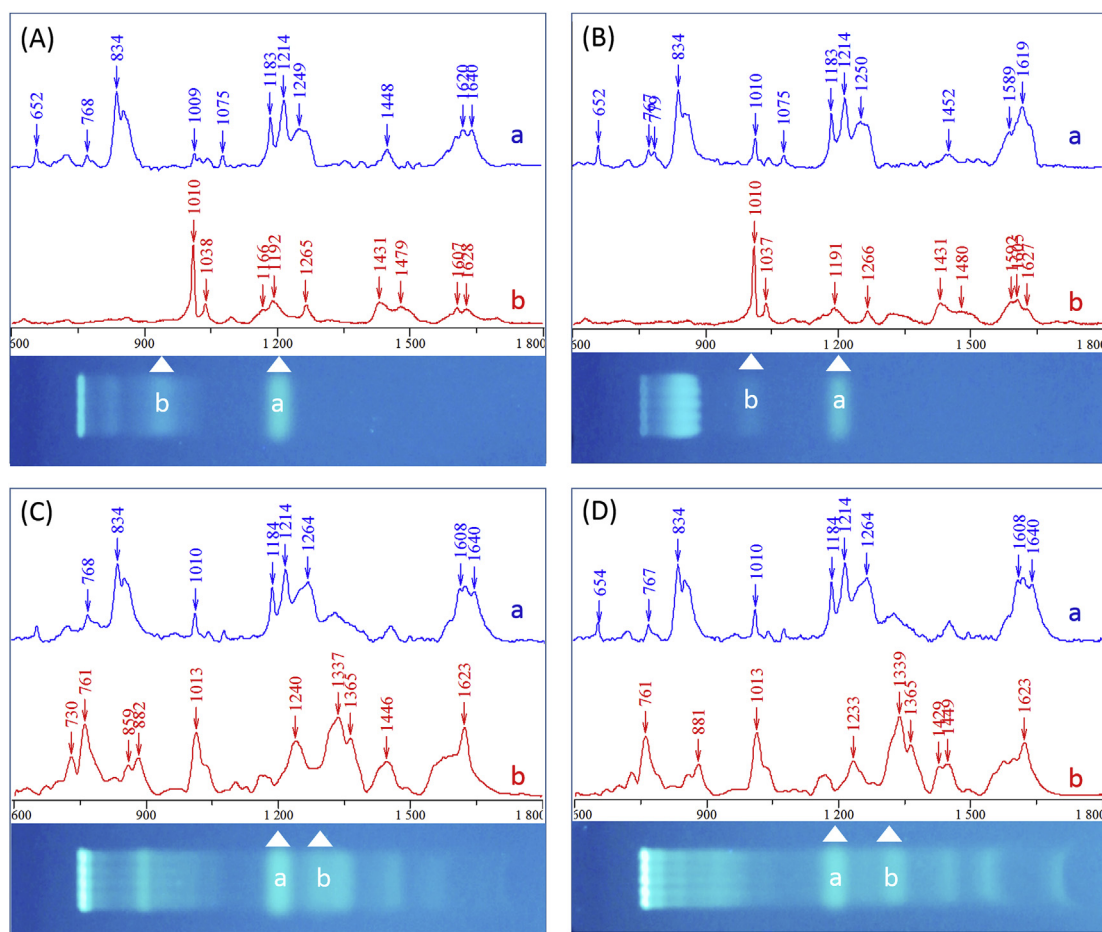


**Fig. 4 – Molecule identification of SERS fingerprints of bands within-/out the window space for Tyr. Sample assignments: Cheese sample 1 (A), 2 (B), 3 (C) and 4 (D).**

**Table 2 – Recovery rates of analyte spiked into different cheese matrix.<sup>a</sup>**

Cheese samples	Native level (mg/kg)	Spiked (mg/kg)	Found (mg/kg)	Recovery rate (%)
C1	32.4 ± 1.5	30.0	59.1 ± 2.1	89.0
C2	22.5 ± 0.7	30.0	47.6 ± 2.5	83.7
C3	59.0 ± 1.5	20.0	80.3 ± 2.3	106.5
C4	43.5 ± 2.1	20.0	65.2 ± 1.5	108.5
Blank (water)	0	30.0	28.7 ± 0.8	95.7

<sup>a</sup> Values were calculated from triplicates.

different migration distances. As presented in Fig. 4, the fingerprint patterns of bands within the window space of sample tracks agreed well with that of the reference standard, implying that these positive findings could be unambiguously assigned to Tyr. In contrast, bands outside the window space displayed significantly different spectra profile. After confirmation, the method accuracy was verified by determining the recovery rates of standard spiking. As presented in Table 2, recovery rates were achieved within 83.7–108.5 % in all four investigated cheese samples, indicating that influences from sample matrices to method quantitation was not neglectable, but acceptable from a view of screening purpose.

#### 4. Conclusions

A facile HPTLC-FLD-SERS method tailored for screening Tyr in cheese was established in this study. Steps of the method including preparation, separation, qualification and quantitation showed remarkable convenience and efficiency, compared to their counterparts in HPLC-MS methods. Besides, it was noteworthy that the combination of substrates and salts was not optional but essential for SERS detection on HPTLC plates. Particularly, both the anion and cation moieties of a salt synergistically influenced the detectability of SERS. In this case, the most sensitive and informative SERS fingerprints of Tyr were resulted from jointly using AgNPs, 3 mol/L NaBr and 633 nm excitation.

With the tightening of food safety regulations, implementation work in screening manner posed great challenges to conventional techniques. The most important points in such work were to rapidly obtain reliable identification and quantitation of analyte in highly sophisticated matrix. Therefore, the workflow proposed here may be a good example for these tasks, striking an excellent balance between specificity, sensitivity and simplicity.

#### Conflicts of interest

There were no conflicts of interest.

#### Acknowledgement

This work was financially supported by Natural Science Foundation of Jiangsu Province [BK20170177], Jiangnan University Fundamental Research Funds for the Central Universities [JUSRP116035], China Postdoctoral Science Foundation [2017M610298], National Key Research and Development program [2017YFF0207800 and 2016YFD0400304], and National Natural Science Foundation of China [31471584].

#### Appendix A. Supplementary data

Supplementary data related to this article can be found at <http://dx.doi.org/10.1016/j.jfda.2017.07.007>.

#### REFERENCES

- [1] John J, Reghuwanshi A, Aravind UK, Aravindakumar CT. Development and validation of a high-performance thin layer chromatography method for the determination of cholesterol concentration. *J Food Drug Anal* 2015;23:219–24.
- [2] Patel KG, Shah PM, Shah PA, Gandhi TR. Validated high-performance thin-layer chromatographic (HPTLC) method for simultaneous determination of nadifloxacin, mometasone furoate, and miconazole nitrate cream using fractional factorial design. *J Food Drug Anal* 2016;24:610–9.
- [3] Agrawal P, Laddha K. Development of validated high-performance thin layer chromatography for quantification of aristolochic acid in different species of the Aristolochiaceae family. *J Food Drug Anal* 2017;25:425–9.
- [4] Chear NJ-Y, Khaw K-Y, Murugaiyah V, Lai C-S. Cholinesterase inhibitory activity and chemical constituents of *Stenochlaena palustris* fronds at two different stages of maturity. *J Food Drug Anal* 2016;24:358–66.
- [5] Jyotshna, Srivastava P, Killadi B, Shanker K. Uni-dimensional double development HPTLC-densitometry method for simultaneous analysis of mangiferin and lupeol content in mango (*Mangifera indica*) pulp and peel during storage. *Food Chem* 2015;176:91–8.
- [6] Amoli-Diva M, Pourghazi K. Gold nanoparticles grafted modified silica gel as a new stationary phase for separation and determination of steroid hormones by thin layer chromatography. *J Food Drug Anal* 2015;23:279–86.
- [7] Chen Y, Schwack W. High-performance thin-layer chromatography screening of multi class antibiotics in animal food by bioluminescent bioautography and electrospray ionization mass spectrometry. *J Chromatogr A* 2014;1356:249–57.
- [8] Chen Y, Morlock GE. Layer-induced sensitivity enhancement in planar chromatography–bioluminescence–mass spectrometry: application to alkaloids. *Chromatographia* 2016;79:89–96.
- [9] Zhang L, Shi J, Tang J, Cheng Z, Lu X, Kong Y, et al. Direct coupling of thin-layer chromatography–bioautography with electrostatic field induced spray ionization–mass spectrometry for separation and identification of lipase inhibitors in lotus leaves. *Anal Chim Acta* 2017;967:52–8.
- [10] Hu B, Xin G-z, So P-K, Yao Z-P. Thin layer chromatography coupled with electrospray ionization mass spectrometry for direct analysis of raw samples. *J Chromatogr A* 2015;1415:155–60.
- [11] Cheng S-C, Huang M-Z, Wu L-C, Chou C-C, Cheng C-N, Jhang S-S, et al. Building blocks for the development of an interface for high-throughput thin layer chromatography/ambient mass spectrometric analysis: a green methodology. *Anal Chem* 2012;84:5864–8.
- [12] Adhami H-R, Scherer U, Kaehlig H, Hettich T, Schlotterbeck G, Reich E, et al. Combination of bioautography with HPTLC–MS/NMR: a fast identification of acetylcholinesterase inhibitors from galbanum†. *Phytochem Anal* 2013;24:395–400.
- [13] Li Y-S, Church JS. Raman spectroscopy in the analysis of food and pharmaceutical nanomaterials. *J Food Drug Anal* 2014;22:29–48.
- [14] Li D-W, Qu L-L, Hu K, Long Y-T, Tian H. Monitoring of endogenous hydrogen sulfide in living cells using surface-enhanced Raman scattering. *Angew Chem Int Ed* 2015;54:12758–61.
- [15] Cao Y, Li D-W, Zhao L-J, Liu X-Y, Cao X-M, Long Y-T. Highly selective detection of carbon monoxide in living cells by palladacycle carbonylation-based surface enhanced Raman spectroscopy nanosensors. *Anal Chem* 2015;87:9696–701.

- [16] Stephen Inbaraj B, Chen BH. Nanomaterial-based sensors for detection of foodborne bacterial pathogens and toxins as well as pork adulteration in meat products. *J Food Drug Anal* 2016;24:15–28.
- [17] Fang F, Qi Y, Lu F, Yang L. Highly sensitive on-site detection of drugs adulterated in botanical dietary supplements using thin layer chromatography combined with dynamic surface enhanced Raman spectroscopy. *Talanta* 2016;146:351–7.
- [18] Zhu Q, Chen M, Han L, Yuan Y, Lu F. High efficiency screening of nine lipid-lowering adulterants in herbal dietary supplements using thin layer chromatography coupled with surface enhanced Raman spectroscopy. *Anal Methods* 2017;9:1595–602.
- [19] Linares DM, del Rio B, Redruello B, Ladero V, Martin MC, Fernandez M, et al. Comparative analysis of the in vitro cytotoxicity of the dietary biogenic amines tyramine and histamine. *Food Chem* 2016;197(Part A):658–63.
- [20] Hazards EPoB. Scientific opinion on risk based control of biogenic amine formation in fermented foods. *EFSA J* 2011;9:2393–n/a.
- [21] Restuccia D, Spizzirri UG, Puoci F, Cirillo G, Curcio M, Parisi OI, et al. A new method for the determination of biogenic amines in cheese by LC with evaporative light scattering detector. *Talanta* 2011;85:363–9.
- [22] Lee PC, Meisel D. Adsorption and surface-enhanced Raman of dyes on silver and gold sols. *J Phys Chem* 1982;86:3391–5.
- [23] Vicario A, Sergio V, Toffoli G, Bonifacio A. Surface-enhanced Raman spectroscopy of the anti-cancer drug irinotecan in presence of human serum albumin. *Colloids Surf B* 2015;127:41–6.
- [24] Otto A, Bruckbauer A, Chen YX. On the chloride activation in SERS and single molecule SERS. *J Mol Struct* 2003;661–662:501–14.
- [25] Li D, Qu L, Zhai W, Xue J, Fossey JS, Long Y. Facile on-site detection of substituted aromatic pollutants in water using thin layer chromatography combined with surface-enhanced Raman spectroscopy. *Environ Sci Technol* 2011;45:4046–52.
- [26] Chen X, Gu H, Shen G, Dong X, Kang J. Spectroscopic study of surface enhanced Raman scattering of caffeine on borohydride-reduced silver colloids. *J Mol Struct* 2010;975:63–8.
- [27] Xie Z, Wang Y, Chen Y, Xu X, Jin Z, Ding Y, et al. Tuneable surface enhanced Raman spectroscopy hyphenated to chemically derivatized thin-layer chromatography plates for screening histamine in fish. *Food Chem* 2017;230:547–52.
- [28] Mikac L, Ivanda M, Gotić M, Mihelj T, Horvat L. Synthesis and characterization of silver colloidal nanoparticles with different coatings for SERS application. *J Nanoparticle Res* 2014;16:2748.
- [29] Maher RC. SERS hot spots. In: Kumar GSSR, editor. *Raman spectroscopy for nanomaterials characterization*. Berlin, Heidelberg: Springer Berlin Heidelberg; 2012. p. 215–60.